Zr-Fumarate MOF a Novel CO_2-Adsorbing Material: Synthesis and Characterization

Mani Ganesh[1,2], Pushparaj Hemalatha[1,2], Mei Mei Peng[1,2], Wang Seog Cha[3], Hyun Tae Jang[1,2*]

[1] *Department of Chemical Engineering, Hanseo University, 360 Daegok-ri, Haemi-myun, Seosan-si 356 706, Chungcheongnam-do, Korea*
[2] *Korea Carbon Capture & Sequestration R&D Centre, Seosan-si 356 706, Korea*
[3] *School of Civil and Environmental Engineering, Kunsan National University, Kunsan 573701, Korea*

ABSTRACT

A novel Zr-fumarate (Zr-fum) metal organic framework was synthesized by the reaction of zirconium chloride and fumaric acid under solvothermal conditions without a formic acid modulator. The synthesized material was characterized by the powder X-ray diffraction, Thermogravimetric Analysis (TGA), Scanning Electron Microscopy (SEM), Fourier Transform Infrared Spectroscopy (FT-IR), and Brunauer-Emmett-Teller (BET) techniques. The results of powder XRD showed the presence of amorphous and crystalline phases. The surface area and average pore diameter of the material were found to be 205.49 m^2/g and 2.12 nm, respectively, and TGA showed that the material was stable up to 300°C. The CO_2 adsorption properties of the Zr-fum MOF revealed an uptake of 8 wt% at room temperature (25°C) and atmospheric pressure. The cyclic CO_2 sorption study showed the complete recyclability of the synthesized material, suggesting that the material has potential for use in gas sorption and separation.

Keywords: Zirconium; Fumaric acid; MOF; CO_2 adsorption.

INTRODUCTION

Among the greenhouse gases listed in the Kyoto Protocol on global warming, carbon dioxide (CO_2) is important because its emission is notably high compared to others due to the continuous utilization of fossil fuel for energy production and automobiles (Houghton *et al.*, 2001). This leads to climatic change followed by the destruction of earth's ecological systems (Shirayama, 1998; Seibel and Walsh, 2001; Thistle *et al.*, 2005; Zoback and Gorelick 2012). Control of the utilization of fossil fuel for energy production will be impossible until an effective non-conventional energy source is identified or invented. CO_2 emission should be controlled before it has a high impact on the earth's climate. Much research has been devoted in the last decade to minimize the concentration of CO_2 using liquid and solid sorbents. Mono ethanol amine (MEA) was identified as a potent liquid sorbent for CO_2, but it suffers disadvantages, in that the: energy needed for desorption and corrosion has made them unsuitable for continuous application in commercial plants (Veawab *et al.*, 1999; Soosaiprakasam and Veawab, 2008; Rahman *et al.*, 2012).

Hence, to overcome such drawbacks, the amines were impregnated in porous silicas (Soriano *et al.*, 2009; Zhu *et al.*, 2010). CO_2 capture on solid sorbents such as metal oxides, zeolites, functionalized silicas, and carbon have drawn interest (Lee *et al.*, 2002; Lin *et al.*, 2009; Zhao *et al.*, 2010). In addition, porous polymers with intrinsic microporosity and covalent organic polymers have gained attention due to their high surface area and CO_2-capturing capacity (Budd *et al.*, 2004; Germain *et al.*, 2006; Liu *et al.*, 2008; Ghanem *et al.*, 2010; Bezzu *et al.*, 2012). Metal-organic frameworks (MOFs) or porous coordination polymers are a class of novel materials constructed by metal and an organic ligand through a strong coordination bond. The proper choice of metal centers and organic linkers results in the generation of new MOFs. Their high surface area, high micropore volume, and tunable pore size make them promising candidates in the fields of gas storage and separation (Li *et al.*, 2009; Murray *et al.*, 2009; Zou *et al.*, 2010; Ferey *et al.*, 2011; Llewellyn *et al.*, 2011), catalysis (Xamena *et al.*, 2007; Lee *et al.*, 2009), sensing (Achmann *et al.*, 2009; Iswarya *et al.*, 2012), and drug delivery (Horcajada *et al.*, 2008; Rieter *et al.*, 2008; Taylor-Pashow *et al.*, 2009). Yaghi's group reported several MOFs with ultra-high porosity (Furukawa *et al.*, 2010). Cavka *et al.* (2008) synthesized Zr-MOF: UiO-66, UiO-67 and UiO-68 using 1,4-benzene-dicarboxylate, biphenyl-dicarboxylate, and terphenyl dicarboxylate as linkers, respectively. The reported

---

[*] Corresponding author.

E-mail address: htjang@hanseo.ac.kr

Ganesh et al., Aerosol and Air Quality Research, 14: 1605–1612, 2014

MOF possesses high surface area and exceptional stability. The Zr-O bonds within the SBUs of Zr-MOFs contribute to the enhanced stability. Upon considering the key features of Zr-based MOF, Cmarik *et al.* (2012) functionalized UiO-66 with -NH_2, -NO_2, -OMe, and -Naphthyl groups, and examined their CO_2 adsorption capability as a function of pressure. The presence of polar functional groups significantly increased the adsorption than non-polar groups. Among them, UiO-66–NH_2 shows the highest adsorption with high CO_2/CH_4 and CO_2/N_2 selectivity.

Isoreticular metal organic framework-1 (IRMOF-1) is a class of MOF constructed by connecting Zn_4O clusters with terephalate linkers (Liu *et al.*, 2012). These IRMOFs have been reported to exhibit good CO_2 sorption capability. Replacement of the linker in IRMOFs with a cost-effective fumarate led to a new non-interpenerated IRMOF with high rigidity and porosity. High-pressure gas sorption measurements revealed that the Zn_4O $(FMA)_3$ MOF could adsorb 69 wt% of CO_2 at 300 K (27°C) and 28 bar (Xue *et al.*, 2009). Recently, Wißmann's group suggested that varying the concentration of the modulator in the synthesis of UiO-66 and UiO-67 results in MOF with different morphologies (Wißmann *et al.*, 2012). In addition, they synthesized a novel Zr-based metal-organic framework (MOF) with fumarate (fum) dianions as linkers with and without formic acid, a monocarboxylic modulator. The topology of the Zr-fumarate was similar to that of UiO-66 but has a primitive cubic lattice instead of a face-centered lattice. In the absence of the modulator, an amorphous phase is obtained, while the addition of only 0.5 eq of the modulator led to the production of small reflections of crystalline phase along with the amorphous phase. The addition of more than 5 eq of modulator resulted in materials with a highly crystalline phase. In this regard, we re-synthesized Zr-fum MOF without the modulator and examined its CO_2 adsorption properties at first time.

EXPERIMENTAL

Materials

Zirconium (IV) chloride ($ZrCl_4$) was obtained from Sigma Aldrich. Fumaric acid, solvents, N,N-dimethylformamide (DMF), chloroform, and ethanol were purchased from Daejung Chemicals & Metals and used as received without any purification.

Synthesis of Zr-fum MOF

Synthesis was carried out using a reported procedure (Wißmann *et al.*, 2012) without a formic acid modulator. In a typical synthesis, fumaric acid (1.55 mmol) was dissolved in 20 mL of DMF, and 0.517 mmol $ZrCl_4$ was added to it with stirring. Then, the mixture was transferred to a Teflon-lined stainless-steel autoclave and heated at 120°C for 24 h. It was then allowed to cool to room temperature naturally. The obtained white solid was filtered, washed several times with DMF and ethanol to remove unreacted materials, and finally dried in an oven at 70°C for 24 h. After exchanging with $CHCl_3$ thrice at 12-h intervals, the product was dried at 100°C in vacuum to yield Zr-fum MOF.

Characterization

The synthesized Zr-fum MOF was characterized by X-ray diffraction (XRD) on a Rigaku Miniflex diffractometer using CuKα radiation (λ = 1.54 Å). The diffraction data were recorded in the 2θ range of 5–80° with a 0.1° step size and a 1-s step time. A SCINCO thermogravimeter N-1000 analyzer was used to study the thermal stability of the material. A sample weighing *ca.* 10 mg was loaded into a platinum sample pan of the TG unit, and the temperature was programmed to attain 800°C at 10 °C/min rate in nitrogen atmosphere. A JEOL-JSM 5600 scanning electron microscope (SEM) was used to study the morphology after sputtering with gold plasma with a sputter coater (Cressington, Sputter Coater-108 auto). A BELSORP mini II volumetric adsorption analyzer was used for the nitrogen adsorption-desorption isotherm measurements at –196°C. The samples were evacuated at 150°C before each adsorption experiment. The specific surface area was determined from the linear part of the BET equation. The pore volume was calculated using the BET plot from the amount of nitrogen gas adsorbed at the last adsorption point (p/p_0 = 0.99). The synthesized material was examined by Fourier Transform Infrared (FTIR) spectroscopy by scanning 20 times at 4 cm^{-1} resolution in the range of 4000–400 cm^{-1} on a Nicolet IR 200 spectrometer after pelletizing with KBr.
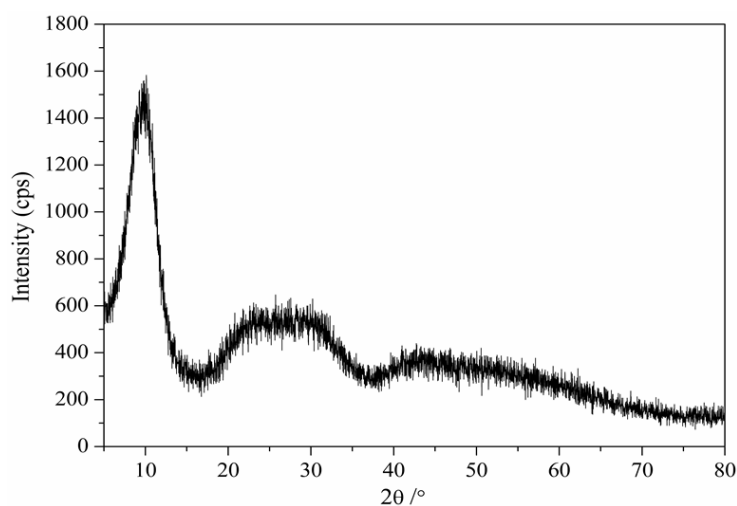
CO_2 Adsorption

CO_2 adsorption-desorption measurements using high-purity CO_2 (99.99%) and N_2 for the samples were performed using TGA. A sample weight of ca. 10 mg was loaded into a platinum sample pan in a TG unit, and the initial activation was carried out at 150°C for 1 h under N_2 atmosphere. Then, the temperature of the sample was brought down to 25, 50, or 75°C for CO_2 adsorption. The desorption was conducted by gradually raising the temperature from 25, 50, or 75°C to 150°C by passing N_2. CO_2 and N_2 were passed through an automatic valve assisted by a timer for continuous adsorption or desorption profiles, respectively. Further selectivity tests were carried using 15% CO_2 gas with N_2 as a makeup gas. A recyclability test was carried at 25°C using 99.99% pure CO_2 for three cycles. Effect of moisture was carried after exposing the material to 20% RH for 24 h and then same procedure repeated for CO_2 adsorption.

RESULTS AND DISCUSSION

Characterization

The XRD pattern of Zr-fum MOF is depicted in Fig. 1. The peaks between 5–10° and 20–30° (2θ) were observed in addition to an amorphous phase. These peaks may be due to the partial crystallization of MOF even without the modulator. The intensity of the peaks was higher than reported in the literature (Wißmann *et al.*, 2012). Fig. 2 illustrates the N_2 adsorption-desorption isotherm of Zr-fum MOF. It belonged to Type-I adsorption isotherm characteristics for microporous materials with a monolayer volume of 47.21 cm^3/g. The surface area and average pore diameter were found to be 205.49 m^2/g and 2.12 nm, respectively. The surface area was lower than that reported for Zr-fumarate in the presence of

Fig. 1. XRD pattern of Zr-fum MOF.
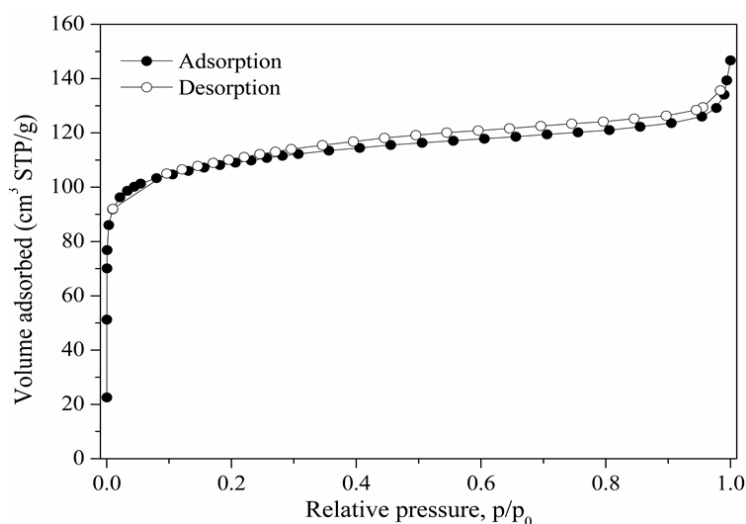
Fig. 2. Nitrogen adsorption-desorption isothermals of Zr-fum MOF.

formic acid (856 m^2/g) (Wißmann *et al.*, 2012). Hence, the presence of formic acid plays a key role by hastening the formation of the crystalline phase. In addition to micropores, the presence of small hysteresis pertaining to mesopores was also observed. The formation of micropores facilitated the sorption of CO_2 by the material, as discussed below. The SEM image is depicted in Fig. 3. No definite shape of the crystals was observed. Due to the absence of the modulator, the extent of agglomeration increased in the present study.

The thermal stability of Zr-fum MOF was studied using TGA (Fig. 4). The synthesized material showed a continuous weight loss up to 425°C. The initial weight loss of 5–10% until 140°C was attributed to the loss of solvent occluded in the pores of the material. The successive major weight loss starts to begin above 260°C and extent up to 400°C which displays the loss of organic linker, fumaric acid. This weight loss pattern was similar with that of Wißmann *et al.* (2012) report. The final residual weight was 58.04%. Fig. 5 depicts the FTIR spectrum of the synthesized MOF. The spectrum shows two characteristic bands of the carboxylate
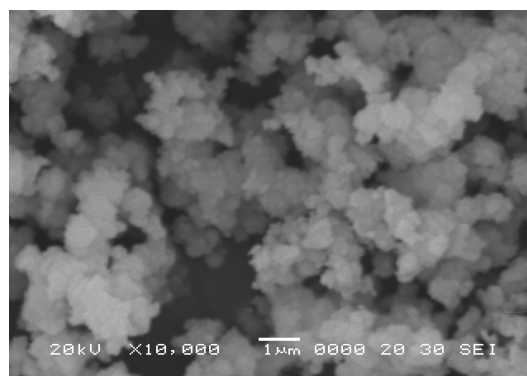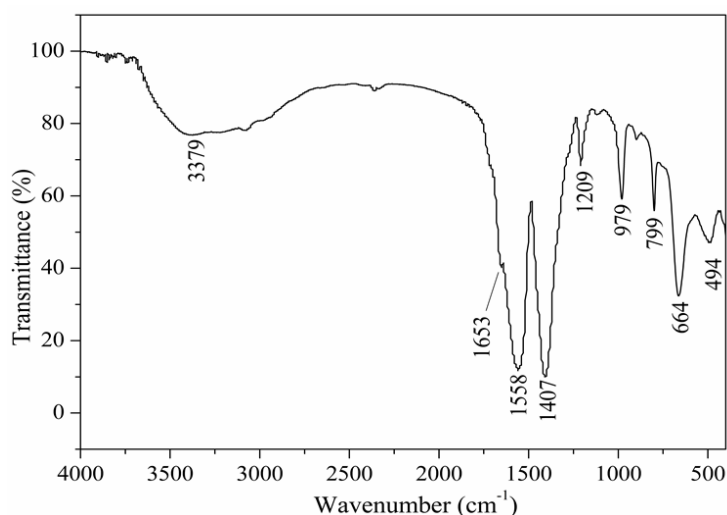

Fig. 3. SEM image of Zr-fum MOF.

groups (COO-) between 1300 and 1600 cm^{-1}. Asymmetrical stretching occurred at 1558 cm^{-1} with stretching at 1407 cm^{-1}. The appearance of new medium-intensity band at 494 cm^{-1} is attributed to Zr-O stretching vibration (Mishra and Singh, 2004).
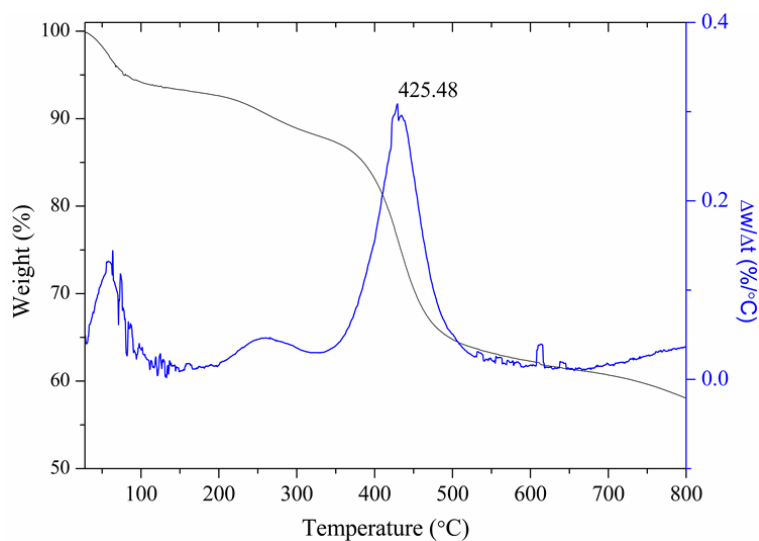
Fig. 4. Thermogram of Zr-fum MOF.

**Fig. 5.** FTIR spectrum of Zr-fum MOF.

CO$_2$ Adsorption

Fig. 6 depicts the CO$_2$ continuous adsorption-desorption profiles of Zr-fum MOF at various temperatures (25, 50, and 75°C). The initial activation of the material was carried out at 150°C in order to remove the solvent occluded in the pores. A maximum CO$_2$ uptake of about 8 wt% (1.818 mmol/g) was observed at 25°C and 1 bar, while it decreased at 50 and 75°C. The decrease in adsorption was due to the decrease in adsorbent-adsorbate interactions (site-adsorbate) induced by an increase of the mobility of adsorbate into the sorbent as a result of the rise of thermal agitation. Cmarik *et al.* (2012) reported that among the amino-, nitro-, methoxy-, and naphthyl-functionalized UiO-66, UiO-66-NH$_2$ showed a maximum CO$_2$ uptake of about 8.406 mol/kg (25°C, 19.989 bar). The presence of polar functional groups increased the sorption when compared to the non-polar groups. The lowering of CO$_2$ uptake in the nitro- and methoxy-functionalized UiO-66 was attributed to decreases in the surface area and pore volume due to the bulkier moieties.

The presence of naphthyl groups still reduces the sorption capability due to greater molar mass, smaller pore volume, steric hindrance near the metal cluster, and a lack of significantly stronger surface binding sites. Zn$_4$O (FMA)$_3$ exhibited a CO$_2$ storage of 69 wt% (15.68 mmol/g) at a pressure of 28 bar (Xue *et al.*, 2009). In comparison with the results of previously reported Zr-MOF, the Zr-fum MOF synthesized in the present work showed a high CO$_2$ sorption capacity at atmospheric pressure. Zn and Zr based MOF showed high adsorption only at high pressure, hence they are for pressure swing adsorption.

The results of cyclical CO$_2$ sorption study of Zr-fum MOF are illustrated in Fig. 7. The CO$_2$ sorption capacity (8 wt% at 25°C, 1 bar) remains unchanged for more than five cycle, showed physisorption-based processes in the material. Hence, the material not only possesses a low-temperature capturing capability, but also displayed a perfect recycling property. In addition, complete regeneration was observed when the temperature was increased from 25 to 150°C.
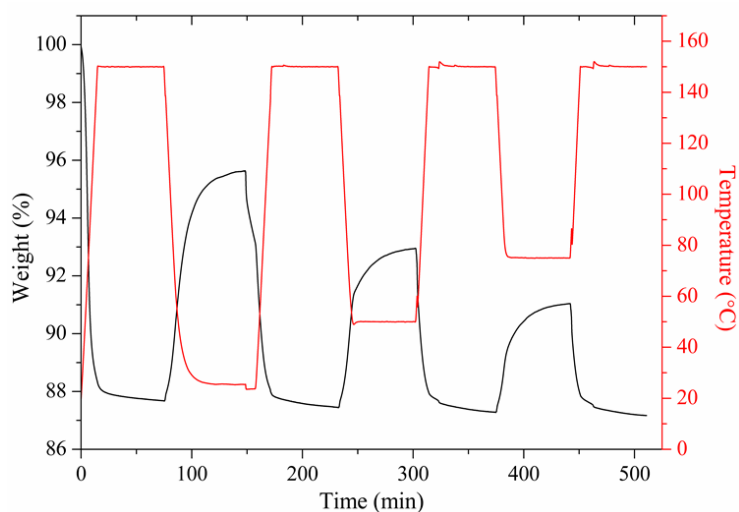
Fig. 6. CO_2 adsorption-desorption profiles of Zr-fum MOF at 25, 50 and 75°C.
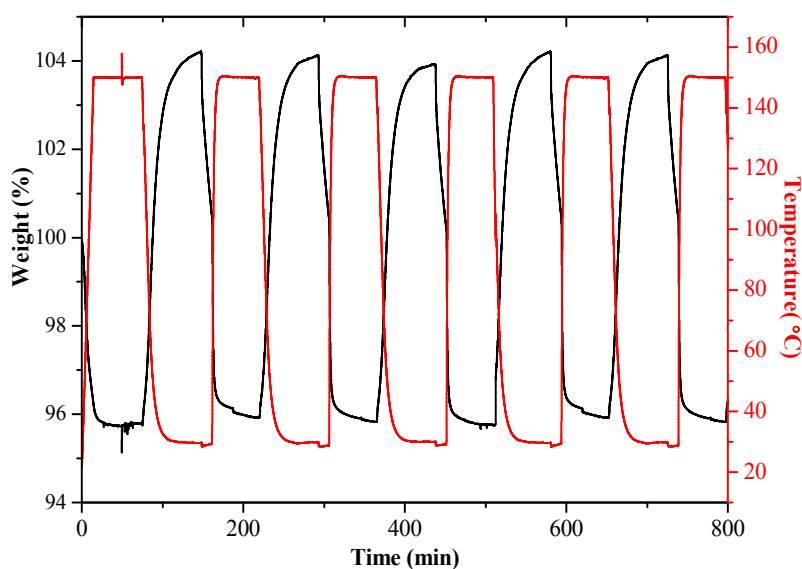

Fig. 7. CO_2 cyclic profile of Zr-fum MOF at 25°C (adsorption) and 150°C (desorption).

Furthermore, the adsorption study was carried out using 15% CO_2 in N_2 gas (Fig. 8), a condition in flue gas processing. There was reduction in the CO_2 uptake of about 50%. Based on the crystal structural study by Wißmann *et al.* (2012) reported that the topology of the structure of UiO-66 is retained in the structure of Zr-fum, i.e., Zr_6O_4 $(OH)_4(O_2C)_{12}$ clusters are positioned at the corners and the faces of a cube and are interconnected to other SBUs by 12 linkers but it loses its FCC structured by the kinked geometry of the fumarate linkers, the Zr-O clusters are tilted into different directions. Further there is evidence resorted for the presence of open metal centers. Hence the possible mechanism of adsorption could be micro pore filling by molecular breathing as reported for other microporous metal organic frameworks. Further, the results of CO_2 adsorption by 20% humidity exposed MOF showed about 13.5 wt% (Fig. 9) this enhancement may be due to coordinated water on metal site on the surface. Hence it could be concluded

that the water molecule coordinated on the moisture exposed sample may enhanced the adsorption by hydrogen bonding as stated in other reports (Liu *et al.*, 2012). Further systematic studies on the same is planned to conduct in near future.

CONCLUSIONS

Zr-fum MOF was successfully synthesized without a formic acid modulator and examined for CO_2 adsorption. The synthesized material was stable at up to 300°C. The amount of physisorbed CO_2 at 25°C and 1 bar of pressure was 8 wt% (1.818 mmol/g). Zr-fum MOF could be easily regenerated after CO_2 adsorption and recycled. An important observation was low-temperature adsorption and desorption in the synthesized Zr-fum MOF. In addition, very cheap fumaric acid was used as the organic linker for the synthesis of the Zr-fum MOF. This study could be extended to other MOF with a proper choice of metal and fumaric acid as the
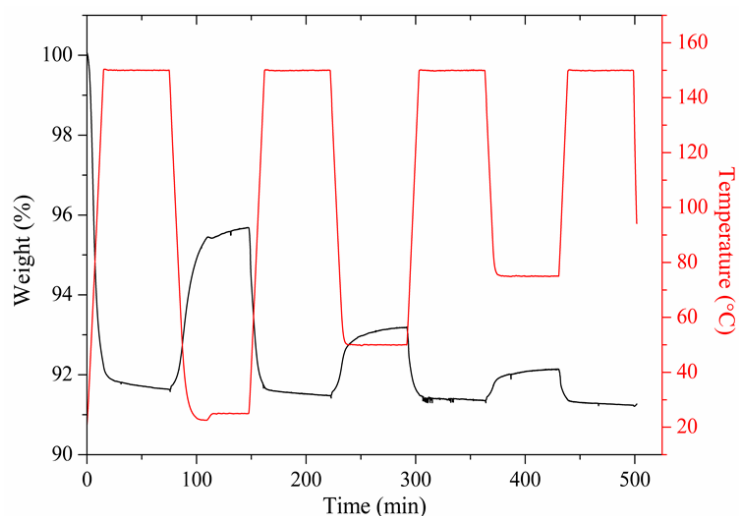
Fig. 8. CO_2 adsorption-desorption profile of Zr-fum MOF using CO_2 (15% in N_2)**.**
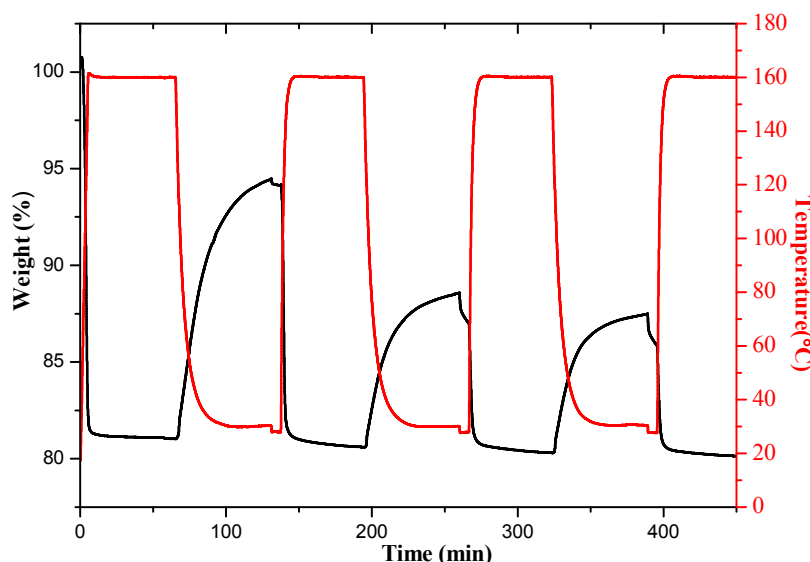
Fig. 9. CO_2 adsorption-desorption profile of Zr-fum MOF using after exposing to 20% humidity (moisture effect).

linker. Hence, it is concluded that the synthesized Zr-fum MOF could be used as a sorbent for the post-combustion capture and storage of CO_2.

ACKNOWLEDGEMENTS

REFERENCES

Abid, H.R., Pham, G.H., Ang, H.M., Tade, M.O. and Wang, S. (2012). Adsorption of CH_4 and CO_2 on Zr-metal Organic Frameworks. *J. Colloid Interface Sci.* 366: 120–124.

Achmann, S., Hagen, G., Kita, J., Malkowsky, I.M., Kiener, C. and Moos, R. (2009). Metal-organic Frameworks for Sensing Applications in the Gas Phase. *Sensors* 9: 1574–1589.

Bezzu, C.G., Carta, M., Tonkins, A., Jansen, J.C., Bernardo, P., Bazzarelli, F. and McKeown, N. B.A. (2012). Spirobifluorene-based Polymer of Intrinsic Microporosity with Improved Performance for Gas Separation. *Adv. Mater.* 24: 5930–5933.

Budd, P.M., Ghanem, B.S., Makhseed, S., McKeown, N.B., Msayib, K.J. and Tattershall, C.E. (2004). Polymers of Intrinsic Microporosity (PIMs): Robust, Solution-processable, Organic Nanoporous Material. *Chem. Commun.* 230–231.

Cavka, J.H., Jakobsen, S., Olsbye, U., Guillou, N., Lamberti, C., Bordiga, S. and Lillerud, K.P. (2008). A New Zirconium Inorganic Building Brick Forming Metal Organic Frameworks with Exceptional Stability. *J. Am. Chem. Soc.* 130: 13850–13851.

Cmarik, G.E., Kim, M., Cohen, S.M. and Walton, K.S.

(2012). Tuning the Adsorption Properties of UiO-66 via Ligand Functionalization. *Langmuir* 28: 15606–15613.

Ferey, G., Serre, C., Devic, T., Maurin, G., Jobic, H., Llewellyn, P.L., De Weireld, G., Vimont, A., Daturi, M. and Chang, J.S. (2011). Why Hybrid Porous Solids Capture Greenhouse Gases? *Chem. Soc. Rev.* 40: 550–562.

Furukawa, H., Ko, N., Go, Y.B., Aratani, N., Choi, S.B., Choi, E., Yazaydin, A.O., Snur, R.Q., O'Keeffe, M., Kim, J. and Yaghi, O.M. (2010). Ultra-high Porosity in Metal-organic Frameworks. *Science* 329: 424–428.

Germain, J., Hradil, J., Fréchet, J.M.J. and Svec, F. (2006). High Surface Area Nonporous Polymers for Reversible Hydrogen Storage. *Chem. Mater.* 18: 4430–4435.

Ghanem, B.S., Hashem, M., Harris, K.D.M., Msayib, K.J., Xu, M., Budd, P.M., Chaukura, N., Book, D., Tedds, S., Walton, A. and McKeown, N.B. (2010). Triptycene-based Polymers of Intrinsic Microporosity: Organic Materials that Can be Tailored for Gas Adsorption. *Macromolecules* 43: 5287–5294.

Horcajada, P., Serre, C., Maurin, G., Ramsahye, N.A., Balas, F., Vallet-Regí, M., Sebban, M., Taulelle, F. and Férey, G. (2008). Flexible Porous Metal-organic Frameworks for a Controlled Drug Delivery. *J. Am. Chem. Soc.* 130: 6774–6780.

Houghton, J.T., Ding, Y., Griggs, D.J., Noguer, M., Linden, P.J.V. and Dai, X (2001). Climate Change 2001: The Scientific Basis. Contribution of Working Group I to the Third Assessment Report of the Intergovernmental Panel on Climate Change, Cambridge University Press, United Kingdom, p. 881.

Iswarya, N., Kumar, M.G., Rajan, K.S. and Rayappan, J.B.B. (2012). Metal Organic Framework (MOF-5) for Sensing of Volatile Organic Compounds. *J. Appl. Sci.* 12: 1681–1685.

Lee, J.S., Kim, J.H., Kim, J.T., Suh, J.K., Lee, J.M. and Lee, C.H. (2002). Adsorption Equilibria of CO$_2$ on Zeolite 13X and Zeolite X/activated Carbon Composite. *J. Chem. Eng. Data* 47: 1237–1242.

Lee, J.Y., Farha, O.K., Roberts, J., Scheidt, K.A., Nguyen, S.T. and Hupp, J.T. (2009). Metal-organic Framework Materials as Catalysts. *Chem. Soc. Rev.* 38: 1450–1459.

Li, J.R., Kuppler, R.J. and Zhou, H.C. (20090. Selective Gas Adsorption and Separation in Metal-organic Frameworks. *Chem. Soc. Rev.* 38: 1477–1504.

Lin, Y.S., Yang, Q. and Ida, J. (20090. High Temperature Sorption of Carbon Dioxide on Perovskite Type Metal Oxides. *J. Taiwan Inst. Chem. Eng.* 40: 276–280.

Liu, J., Thallapally, P.K., McGrail, B.P., Brown, D.R. and Liu, J. (20120. Progress In adsorption-based CO$_2$ Capture by Metal-organic Frameworks. *Chem. Soc. Rev.* 41: 2308–2322.

Liu, Q.Q., Wang, L., Xiao, A.G., Yu, H.J. and Tan, Q.H. (2008). A Hyper-cross-linked Polystyrene with Nano-pore Structure. *Eur. Polym. J.* 44: 2516–2522.

Liu, Y., Wang, Z.U. and Zhou, H.C. (2012). Recent Advances in Carbon Dioxide Capture with Metal-organic Frameworks. *Greenhouse Gases Sci. Technol.* 2: 239–259.

Llewellyn, P.L., Bourrelly, S., Serre, C., Vimon, A., Daturi, M., Hamon, L., Weireld, G.D., Chang, J.S., Hong, D.Y.,

Hwang, Y.K., Jhung, S.H. and Férey, G. (2008). High Uptakes of CO$_2$ and CH$_4$ in Mesoporous Metal Organic Frameworks MIL-100 and MIL-10. *Langmuir* 24: 7245–7250.

Mishra, S. and Singh, A. (2004). Synthesis and Spectroscopic Studies of Homo- and Heteroleptic *N*-aryl Salicylaldiminates of Titanium(IV), Zirconium(IV) and Chromium(III). *Transition Met. Chem.* 29: 164–169.

Murray, L.J., Dinc, M. and Long, J.R. (2009). Hydrogen Storage in Metal-organic Frameworks. *Chem. Soc. Rev.* 38: 1294–314.Rahman, M.H., Bouteldja, H., Fongarland, P., Siaj, M. and Larachi, F. (2012). Corrosion Behavior of Carbon Steel in Alkanolamine/Room-temperature Ionic Liquid Based CO$_2$ Capture Systems. *Ind. Eng. Chem. Res.* 51: 8711–8718.

Rieter, W.J., Pott, K.M., Taylor, K.M.L. and Lin, W.B. (2008). Nanoscale Coordination Polymers for Platinum-based Anticancer Drug Delivery. *J. Am. Chem. Soc.* 130: 11584–11585.

Seibel, B.A. and Walsh, P.J. (2001). Potential Impacts of CO$_2$ Injection on Deep-sea Biota. *Science* 294: 319–320.

Shirayama, Y. (1998). Biodiversity and Biological Impact of Ocean Disposal of Carbon Dioxide. *Waste Manage.* 17: 381–384.

Soosaiprakasam, I.R. and Veawab, A. (2008). Corrosion and Polarization Behavior of Carbon steel in MEA-based CO$_2$ Capture Process. *Int. J. Greenhouse Gas Control* 2: 553–562.

Soriano, A.N., Doma, Jr.B.T. and Li, M.H. (2009). Carbon Dioxide Solubility in Some Ionic Liquids at Moderate Pressures. *J. Taiwan Inst. Chem. Eng.* 40: 387–393.

Taylor-Pashow, K.M., Rocca, J.D., Xie, Z., Tran, S. and Lin, W. (2009). Postsynthetic Modifications of Iron-carboxylate Nanoscale Metal-organic Frameworks for Imaging and Drug Delivery. *J. Am. Chem. Soc.* 131: 14261–14263.

Thistle, D., Carman, K.R., Sedlacek, L., Brewer, P.G., Fleeger, J.W. and Barry, J.P. (2005). Deep-Ocean, Sediment-dwelling Animals are Sensitive to Sequestered Carbon Dioxide. *Mar. Ecol. Prog. Ser.* 289: 1–4.

Veawab, A., Tontiwachwuthikul, P. and Chakma, A. (1999). Corrosion Behavior of Carbon Steel in the CO$_2$ Absorption Process Using Aqueous Amine Solutions. *Ind. Eng. Chem. Res.* 38: 3917–3924.

Wißmann, G., Schaate, A., Lilienthal, S., Bremer, I., Schneider, A.M. and Behrens, P. (2012). Modulated Synthesis of Zr-fumarate MOF. *Microporous Mesoporous Mater.* 152: 64–70.

Xamena, F.X.L., Abad, A., Corma, A. and Garcia, H. (2007). MOFs as Catalysts: Activity, Reusability and Shape-selectivity of a Pd-containing MOF. *J. Catal.* 250: 294–298.

Xue, M., Liu, Y., Schaffino, R.M., Xiang, S., Zhao, X., Zhu, G.S., Qiu, S.L. and Chen, B. (2009). New Prototype Isoreticular Metal-organic Framework Zn$_4$O(FMA)$_3$ for Gas Storage. *Inorg. Chem.* 48: 4649–4651.

Zhao, G., Aziz, B. and Hedin, N. (2010). Carbon Dioxide Adsorption on Mesoporous Silica Surfaces Containing Amine-like Motifs. *App. Energy* 87: 2907–2913.

Zhu, T., Yang, S., Choi, D.K. and Row, K.H. (2010). Adsorption of Carbon Dioxide Using Poly Ethyleneimine Modified Silica Gel. *Korean J. Chem Eng.* 27: 1910–1915.

Zoback, M.D. and Gorelick, S.M. (2012). Earthquake Triggering and Large-scale Geologic Storage of Carbon Dioxide. *Proc. Nat. Acad. Sci. U.S.A.* 109: 10164–10168.

Zou, Y.Q., Abdel-Fattah, A.I., Xu, H.W., Zhao, Y.S. and Hickmott, D.D. (2010). Storage and Separation Applications of Nanoporous Metal-organic Frameworks. *Cryst. Eng. Comm* 12: 1337–1353.